Available online at www.sciencedirect.com
SCIENCE DIRECT
Biochemical and Biophysical Research Communications 342 (2006) 323–329
BBRC
www.elsevier.com/locate/ybbrc

Structural insights into the catalytic mechanism of sphingomyelinases D and evolutionary relationship to glycerophosphodiester phosphodiesterases

Mário T. Murakami [a], Matheus Freitas Fernandes-Pedrosa [b], Sonia A. de Andrade [b], Azat Gabdoulkhakov [c], Christian Betzel [d], Denise V. Tambourgi [b,e,*], Raghuvir K. Arni [a,e,*]

[a] *Department of Physics, IBILCE/UNESP, São José do Rio Preto-SP, Brazil*
[b] *Immunochemistry Laboratory, Butantan Institute, São Paulo-SP, Brazil*
[c] *Institute for Protein Research RAS, Moscow, Russia*
[d] *Division of Biochemistry and Molecular Biology, Hamburg University, Germany*
[e] *Center for Applied Toxinology, Butantan Institute, São Paulo-SP, Brazil*

Received 14 January 2006
Available online 3 February 2006

Abstract

Spider venom sphingomyelinases D catalyze the hydrolysis of sphingomyelin via an Mg^{2+} ion-dependent acid–base catalytic mechanism which involves two histidines. In the crystal structure of the sulfate free enzyme determined at 1.85 Å resolution, the metal ion is tetrahedrally coordinated instead of the trigonal–bipyramidal coordination observed in the sulfate bound form. The observed hyperpolarized state of His47 requires a revision of the previously suggested catalytic mechanism. Molecular modeling indicates that the fundamental structural features important for catalysis are fully conserved in both classes of SMases D and that the Class II SMases D contain an additional intra-chain disulphide bridge (Cys53–Cys201). Structural analysis suggests that the highly homologous enzyme from *Loxosceles bonetti* is unable to hydrolyze sphingomyelin due to the 95Gly → Asn and 134Pro → Glu mutations that modify the local charge and hydrophobicity of the interfacial face. Structural and sequence comparisons confirm the evolutionary relationship between sphingomyelinases D and the glicerophosphodiester phosphoesterases which utilize a similar catalytic mechanism.

Keywords: Sphingomyelinase D; Catalytic mechanism; Mg^{2+}-binding site; Hydrodynamic behavior; Crystal structure; Glycerophosphodiester phosphodiesterases

Sphingomyelinases D (SMases D) (sphingomyelin phosphodiesterase D; E.C. 3.1.4.41) catalyze the hydrolysis of sphingomyelin resulting in the formation of ceramide 1-phosphate (C1P) and choline or the hydrolysis of lysophosphatidyl choline, generating the lipid mediator lysophosphatidic acid (LPA) [1]. C1P is implicated in the stimulation of cell proliferation via a pathway that involves inhibition of acid sphingomyelinase and the simultaneous blocking of ceramide synthesis [2]. LPA is known to induce various biological and pathological responses such as platelet aggregation, endothelial hyperpermeability, and pro-inflammatory responses by signaling through three G-protein-coupled receptors [3,4]. SMases D, the main components of spider venoms of the genus *Loxosceles*, induce severe local dermonecrosis, acute renal failure, thrombocytopenia, platelet aggregation, and systemic intravascular haemolysis, which, in rare cases, lead to death [5].

Surprisingly, SMase D activity is not encountered elsewhere in the animal kingdom, but is present in strains of pathogenic *Corynebacterium*. The bacterial and spider venom SMases D possess similar molecular masses

* Corresponding authors. Fax: +55 17 2212240 (R.K. Arni).
E-mail addresses: dvtambourgi@yahoo.com (D.V. Tambourgi), arni@ibilce.unesp.br (R.K. Arni).

0006-291X/$ - see front matter © 2006 Elsevier Inc. All rights reserved.
doi:10.1016/j.bbrc.2006.01.123

(31–35 kDa) but display low sequence identity and are considered to have originated from a common ancestor, the glycerophosphodiester phosphodiesterases (GDPD; E.C. 3.1.4.46). GDPDs are ubiquitous enzymes, encountered in bacteria and eukaryotes, display a wide specificity and are involved in glycerol metabolism since they catalyze the reaction of glycerophosphodiester and water to alcohol and *sn*-glycerol-3-phosphate.

We have recently reported the results of the first crystal structure of a SMase D from *Loxosceles laeta* (SMase I) in the presence of a bound sulfate ion [6] and described the acid–base catalytic mechanism involving two histidine residues, His12 and His47, and the role of the Mg^{2+} ion. We now report the crystal structure of SMase I determined in the absence of the sulfate ion. In the light of which, the previously suggested mechanism has been revised and we extend this mechanism to encompass the structurally related GDPDs that also utilize a similar catalytic mechanism.

Materials and methods

Protein expression and purification. SMase I (GenBank™ Accession No. AY093599) was expressed in *Escherichia coli* strain BL21 as a fusion protein of SMase I with an N-terminal extension containing a His6 tag [7]. Recombinant SMase I was purified from the soluble fraction of cell lysates on a Ni(II)-chelating-Sepharose Fast Flow column (Amersham Biosciences). Recombinant protein was eluted with a buffer solution containing 100 mM Tris–HCl, pH 8.0, 300 mM NaCl, and 0.8 M imidazole and dialyzed against phosphate-buffered saline, pH 7.2 (10 mM sodium phosphate, 150 mM NaCl).

Dynamic light scattering. Dynamic light scattering (DLS) measurements were performed using a DynaPro-801 Instrument (Protein Solutions, Inc., Charlottesville, VA) equipped with a 25 mW, 780 nm solid-state lazer and a peltier cell. The protein samples were prepared at a concentration of 5 mg/mL in 5 mM Hepes buffer, containing 0.02 M NaCl, pH 7.0, at 20 °C and were loaded in a 20 μL quartz flow cell. The scattered photons were detected by an avalanche photodiode at a fixed scattering angle of 90° and 30 measurements were carried out in a time interval of 30 s. The hydrodynamic radii of gyration, molecular masses, and degree of sample polydispersity were calculated based on the autocorrelation function using the manufacturer's software wherein the radius of gyration (R_g) is extrapolated via the Stokes–Einstein equation. The apparent molecular mass was derived from a standard curve of molecular weights versus measured values of the translational diffusion coefficient obtained from a set of calibrated standard values.

Small angle X-ray scattering. Small angle X-ray scattering (SAXS) experiments were performed at the SAS1 beamline, Laboratório Nacional de Luz Síncrotron (LNLS, Campinas, Brazil). To minimize aggregation effects, the protein concentration used was 2 mg/mL and all experiments were conducted at 20 °C. The wavelength was set to 1.48 Å and the sample-to-detector distance was fixed at 1.07 m. The vertical linear-sensitive position detector was translated upwards in relation to the incident beam so that the scattered intensities for higher scattering angles could be measured and three frames with exposure times of 600 s were recorded. Background scattering was measured before and after each protein sample using the corresponding buffer solution (50 mM Hepes, pH 7.0, 150 mM sodium chloride) and this contribution was subsequently subtracted from the protein scattering patterns after normalization and correction. The R_g and intensity values were obtained by utilizing the Guinier approximations and the theoretical R_g values were calculated based on the atomic coordinates of the model using the program CRYSOL [8].

Crystallization and data collection. Crystals of sulfate ion free SMase I were obtained by the hanging-drop vapour-diffusion method. Equal volumes (1 μL) of protein and mother solution were mixed over wells containing 2.4 M trisodium citrate that was titrated to pH 9.0, using a 0.1 M sodium hydroxide solution. Crystals were soaked in the mother solution which additionally contained 25% glycerol as a cryoprotectant and were cooled to 100 K in a nitrogen-gas stream (Oxford Cryosystems). Diffraction intensities were recorded at the Consortium Beamline X13 at HASYLAB/DESY–Hamburg equipped with an imaging plate detector (MAR345). Integration, scaling and merging of the intensities were carried out using DENZO and SCALEPACK [9]. Analysis of the structure factors using SFCHECK [10] indicated a twinning fraction of 0.373. The twin-related reflections (h, $-h-k$, $-l$) were treated using DETWIN [11] and the detwinned data display residual twinning of 0.035 with an overall completeness of 83.5%.

Structure determination and refinement. The crystal structure of the sulfate free form of SMase I was solved by molecular replacement using the atomic coordinates of the sulfate bound form (PDB entry: 1XX1) [6] as a search model and the program AMoRe [12] as implemented in the CCP4 suite of programs. Initial cycles of restrained refinement were carried out by REFMAC5 [13] and non-crystallographic restraints were imposed. The model was inspected and manually adjusted based on the $2F_o-F_c$ and F_o-F_c electron density maps using the programs TURBO FRODO [14] and COOT [15]. In the later cycles, the non-crystallographic restraints were relaxed and individual isotropic $B_{factors}$ were refined. Solvent molecules, added automatically using ARP/wARP [16], were checked by visual inspection and retained by taking hydrogen bonding potential into consideration. The quality of the model was assessed using *PROCHECK* [17], data collection and refinement statistics are presented in Table 1. The structure factors and atomic coordinates have been deposited with the Protein Data Bank and have been assigned the code 2F9R.

Table 1
Data collection and refinement statistics

PDB code	2F9R
Data-collection statistics	
Space group	$P6_5$
Unit-cell parameters (Å)	$a = b = 140.5$, and $c = 113.6$
Resolution range (Å)	20.0 − 1.85 (1.89 − 1.85)
Unique reflections	101,876
Redundancy	6.1 (5.8)
Completeness (%)	93.9 (96.6)
$I/\sigma(I)$	25.5 (5.2)
R_{merge} (%)[a]	5.7 (27.9)
V_M (Å^3 Da^{-1})	2.34
Solvent content (%)	47.04
Refinement statistics	
R_{factor} (%)[b]	18.7
R_{free} value (%)[c]	23.4
No. of protein atoms	9380 (4 × 285 amino acid residues)
No. of solvent molecules	510
No. of Hepes molecules	3
Mean temperature factor (Å^2)[d]	24.2
r.m.s.d. bond lengths (Å)	0.011
r.m.s.d. bond angles (°)	1.340
Ramachandran plot	
Most favored region (%)	89.7
Additionally allowed regions (%)	10.3
Generously allowed regions (%)	0.0
Disallowed regions (%)	0.0

Values in parentheses are for the highest resolution shell.

[a] $R_{merge} = 100 \times \sum|I(h) - \langle I(h)\rangle| / \sum I(h)$, where $I(h)$ is observed intensity and $\langle I(h)\rangle$ is mean intensity of reflection h over all measurements of $I(h)$.

[b] $R_{factor} = 100 \times \sum|F_o - F_c| / \sum(F_o)$ the sums being taken over all reflections with $F/\sigma(F) > 2$ cutoff.

[c] $R_{free} = R_{factor}$ for 5% of the data, which were not included during crystallographic refinement.

[d] B values are average B values for all non-hydrogen atoms.

Molecular modeling. The atomic coordinates of SMase I (PDB Accession code: 1XX1) [6] served as the template for generating structural models of both the active and inactive SMases D from *L. bonetti* by restraint-based modeling as implemented in the MODELLER program [18]. The overall model was improved enforcing the proper stereochemistry using spatial restraints and CHARMM energy terms, followed by conjugate gradient simulation based on the variable target function method [18]. The loops were optimized using ModLoop [19] taking into consideration the satisfaction of spatial restraints, without relying on a database of known protein structures.

Results and discussion

Hydrodynamic behavior of SMases D

DLS experiments indicate that SMase I (Class I) posses a hydrodynamic radius of 3.43 ± 0.03 nm with a corresponding molecular weight of the monomer of approximately 34.2 kDa in solution. The SAXS experiments carried out with the P1 enzyme (Class II) at low protein concentrations in the presence of 150 mM sodium chloride indicate a R_g of 17.4 Å that is in good agreement with the theoretical R_g calculated from the atomic coordinates of the modeled structure using CRYSOL [8] of 17.7 Å. These results indicate that both the enzymes are monomeric in solution and that the dimeric form encountered in the crystal structure of SMase I could represent an artifact as a result of the high protein and salt concentrations used in the crystallization experiments.

Crystal structure of SMase I

The refinement converged to a crystallographic residual of 18.7% ($R_{free} = 23.4\%$), the asymmetric unit comprises of two dimers (285 residues in each monomer), 3 Hepes (4-(2-hydroxyethyl)-1-piperazineethanesulfonic acid) molecules, 4 Mg^{2+} ions, and 510 solvent water molecules. The quality of the model assessed by PROCHECK [17] indicates that all the stereochemical parameters lie within the expected range (Table 1). The Ramachandran diagram [20] indicates that 89.7% of the main-chain dihedral angles of all non-glycine and non-proline residues are located in the energetically most favored regions and only 10.3% lie in the permitted region. Superpositioning of the atomic coordinates of the sulfate free and sulfate bound forms indicates that the flexible loop regions (residues 198–210), which are disordered and are characterized by diffuse electron densities, adopt different conformations.

Overall structure of SMases D

SMase D folds to form a distorted $(\alpha/\beta)_8$ barrel with the insertion of additional β-strands, α-helices, and several connecting loops [6]. The catalytic loop (blue), variable loop (green), and flexible loop (red) along with other short hydrophobic loops form the interfacial face (*i*-face) of the enzyme where the active site is located in a shallow cleft (Fig. 1A). The catalytic loop (residues 46–60) which contains the catalytically important residue, His47, is fully

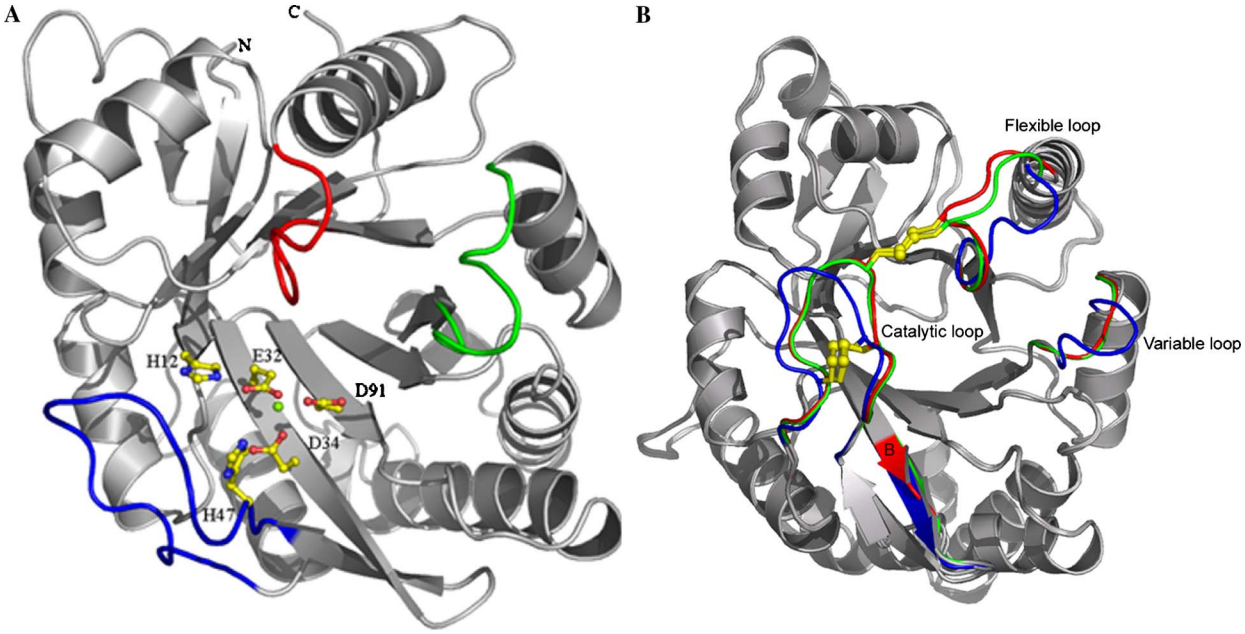

Fig. 1. (A) Ribbon representation of SMase I. The amino acids involved in metal-ion binding and catalysis are presented in atom colors (PDB code: 1XX1, chain A). The catalytic, flexible, and variable loops are colored blue, red, and green, respectively. (B) Differences in the catalytic, flexible, and variable loops in class I (blue), IIa (red), and IIb (green) SMases D. The disulphide bridges are presented by yellow ball and sticks. (For interpretation of the references to color in this figure legend, the reader is referred to the web version of this paper.)

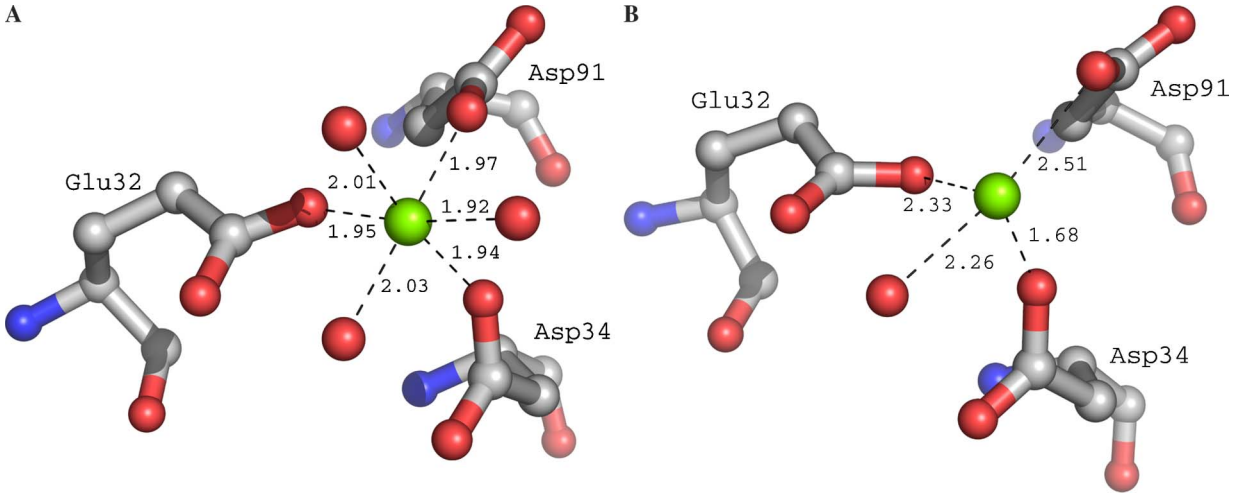

Fig. 2. Coordination sphere of the Mg^{2+} ion (A) in the presence of sulfate ion and (B) in the absence of sulfate ion.

conserved in all SMases D, forms a hairpin due to the presence of a disulphide bridge (Cys51–Cys57) and a network of hydrogen bonds ensures the correct relative orientation of the hairpin with respect to the core of the protein.

Mg^{2+}-binding site

The Mg^{2+}-binding site residues along with Trp230, Ly93, and the two catalytic histidine residues (His12 and His47) form the active-site pocket that is strictly conserved in both spider and bacterial SMases D [6]. In the structure of the sulfate bound SMase I determined at pH 5.5, the Mg^{2+} ion (B_{factor} of ~7.5 Å^2 and a mean Mg–O bond distance of ~2.01 Å) is hexacoordinated by a trigonal–bipyramid formed by the carboxyl oxygens of Glu32, Asp34, Asp91, and three water molecules (Fig. 2A). The latter bind the sulfate ion that is considered to represent the phosphate head group of the sphingomyelin substrate, suggesting a key role for the Mg^{2+} ion in the coordination and stabilization of the phosphonate of sphingomyelin during hydrolysis. In the crystal structure of the sulfate free SMase I determined at pH 9.0, the Mg^{2+} ion is coordinated tetrahedrally by the same three residues (Glu32, Asp34, and Asp91) and a single water molecule (Fig. 2B).

Catalytic mechanism of SMases D

The catalytic mechanism proposed for SMases D based on an acid–base reaction combined with metal ion stabilization [6] involves two histidines, His12 and His47, the former assisted by a hydrogen bond network formed between the carboxylate oxygens of Asp52, Asp233, and Asn252 and the latter by a short bond to Gly48O (distance = 2.7 Å, Figs. 3A and B). In the earlier model, we suggested that His12 functions as the nucleophile that initiates the attack on the scissile phosphodiester bond of the sphingomyelin substrate and His47, after undergoing a rotation of 180° around κ2, functions as the proton donor destabilization a short-lived penta-coordinated covalent intermediate to produce choline [6].

In the structure of SMase I determined in the absence of SO^{4-}, the position previously occupied by a tetrahedral ion is now occupied by a single water molecule which is simultaneously bound to His12 (His12NE2–O = 3.3 Å) and His 47 (His47NE2–O = 2.7 Å) (Fig. 3B). The shorter bond distance observed between His47NE2 and the water molecule indicates that His47 is present in a hyperpolarized state due to the short bond formed between His47ND1 and Gly48O. Thus, indicating that the roles of the two histidines are reversed, i.e., His47 behaves as the nucleophile which initiates the process of hydrolysis by attacking the scissile phosphodiester bond of the substrate, that is subsequently followed by the formation of a short-lived penta-coordinated intermediate. Donation of a hydrogen atom by His12 leads to the formation of choline and the resulting tetrahedral reaction intermediate is stabilized by a covalent bond formed to His47NE2. The previously deprotonated His12 is now able to abstract a proton from a solvent water molecule that initiates a nucleophilic attack on the reaction intermediate, thus resulting in the formation and release of ceramide 1-phosphate followed by a return to the initial state (Fig. 4). In this modified schematic, the energetically highly unfavorable rotation of His47 around κ2 would not be a prerequisite.

Structural classification of SMases D

All spider venom SMases D sequenced to date [8,21,22] display a significant level of sequence homology and thus likely possess the same $(\alpha/\beta)_8$ or TIM barrel fold (Figs. 1A and B). In this family of enzymes, the amino acids essential for metal-ion binding and catalysis are strictly conserved (Fig. 5), however, minor sequence differences result in decreased activity levels or, in the complete absence of hydrolytic activity upon sphingomyelin. Based on the sequence alignment, biochemical and structural

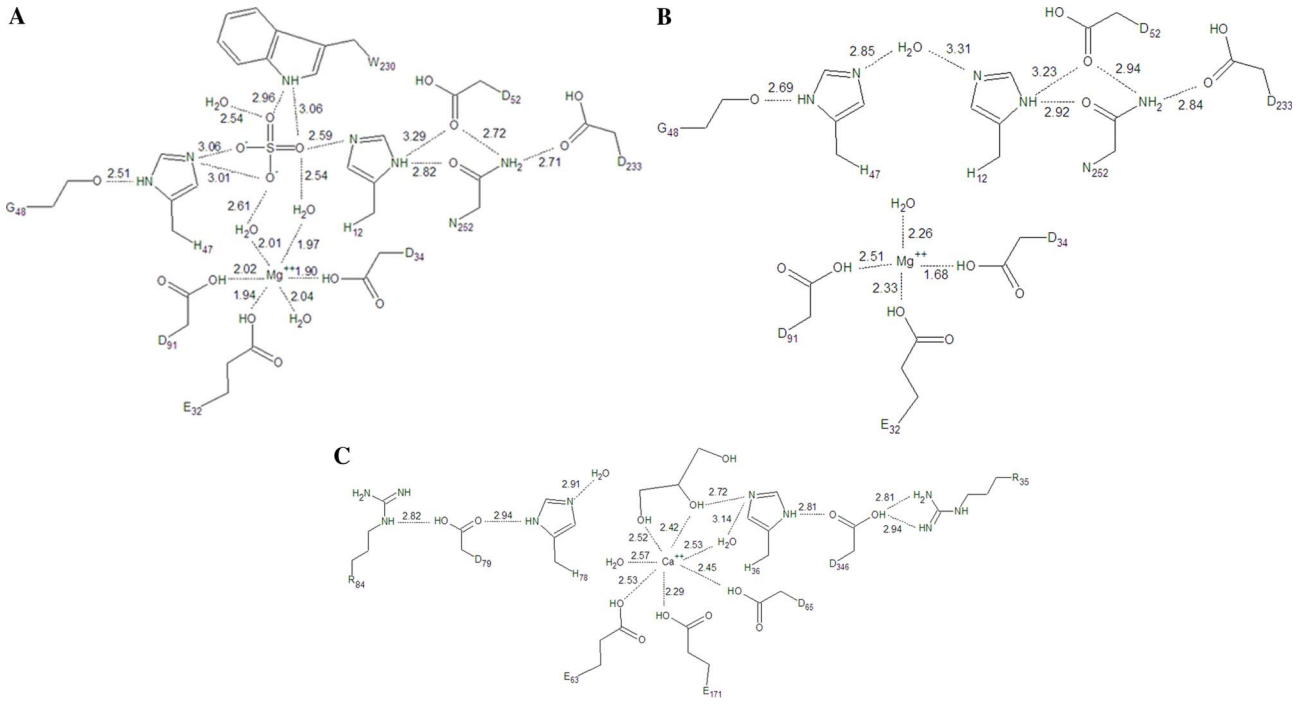

Fig. 3. Network of hydrogen bonds in the active-site pockets of (A) sulfate bound form of SMase I, (B) sulfate free form of SMase I, and (C) GDPD from *Escherichia coli* (PDB code: 1YDY).

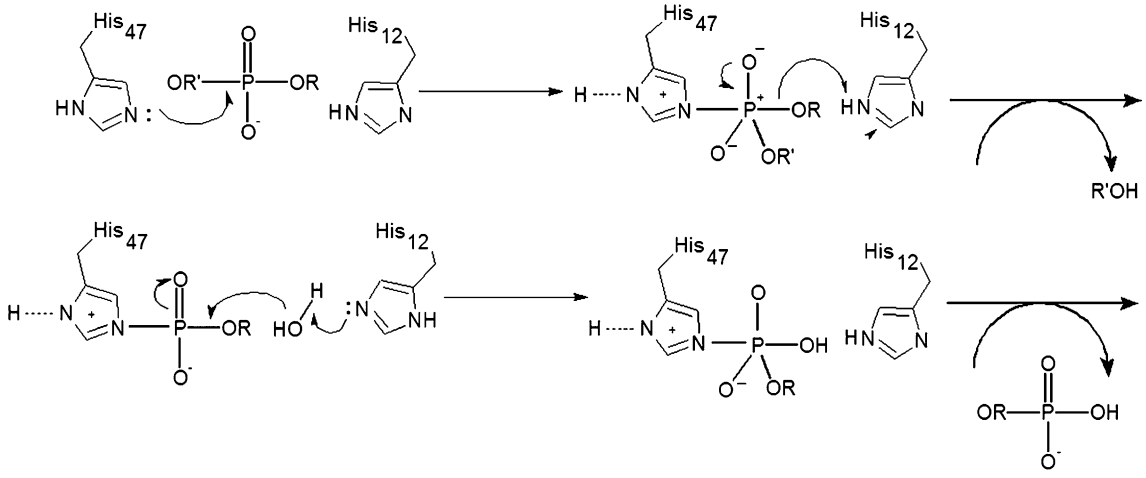

Fig. 4. Catalytic mechanism of SMases D.

data, we propose a classification of spider venom SMases D. The class I enzymes represented by SMase I, a SMase D from *L. laeta* and the H13 isoform possess a single disulphide bridge and contain an extended hydrophobic loop (Fig. 1B; green, amino acid sequence Pro-Tyr-Leu-Pro-Ser). All other SMases D belong to class II, which contains an additional intra-chain disulphide bridge that links the shortened flexible loop (red) with the catalytic loop (blue) (Figs. 1B and 5), and the shortened flexible loop unwinds partially and is involved in dislocating the catalytic loop thus, further shielding the catalytic site.

The class II enzymes can be further subdivided into class IIa and class IIb depending on whether they are capable of hydrolyzing sphingomyelin or not, respectively. In both the class IIa and class IIb SMases D, all the structural elements for metal-ion coordination and catalytic activity are fully conserved, which do not clarify the observed lack of activity of the Class IIb SMases D on sphingomyelin. A detailed structural analysis of a sphere with a radius of 10Å positioned around the active site reveals that all residues important for catalysis are conserved in both sub-classes, except for the dual substitutions at positions 95 (Gly → Asn) and 134 (Pro → Glu), which result in the generation of a hydrophilic environment at the entrance to the active site (Fig. 6) and the presence of a carboxylate group near the active site results in a modification of the local charges maintained mainly by the Mg^{2+} ion. The former region is important in modulating and controlling the approach and also in

```
                1                                                                73
Lb1             -ANKRPAWIMGHM-------VNAIAQIDEFVNLGANSIETDVSFDSSANPEYTYHGIPCDCGRTCTKWENFNDFLVGLRKA
Lb3             --RPKPIWDVAHM-------VNDLELVDEYLGDGANGLELDVAFSDDGTAEKMYHGVPCDCFRSCKRTETFTKYMDYIREL
Smase I         ADNRRPIWNLAHM-------VNAVAQIPDFLDLGANALEADVTFKGSV-PTYTYHGTPCDFGRDCIRWEYFNVFLKTLREY
GDPD            ------VIVLGHRGYSAKYLENTLEAFMKAIEAGANGVELDVRLSKDG-KVVVSHDEDLKRLFGLDVKIRDATVSELKELT
                    74                                                           148
Lb1             ----TTPDDSNYH--EKLILVVFDLKTGSLYDNQAYDAGKKLAKSILQHYWNNGNNGGRAYIVLSIPNLAHYKLITGFKET
Lb3             ----TTPGNSKFN--NNLILLIMDLKLNGIEPNVAYAAGKSVAEKLLSSYWQNGESGARAYIVLSLETITRPEFINGFRDA
SMase I         ----TTPGNAKYR--DGFILFVLDLKTGSLSNDQVRPAGENVAKELLQNYWNNGNNGGRAYVVLSLPDIGHYEFVRGFKEV
GDPD            DGKITTLKEVFENVSDDKIINI-EIKEREAADAVLEIS----------KKRKNLIFSSFDLDLLDEKFKGTKYGYLIDEEN
                149                                                              229
Lb1             LTSDGHPELMDKIGYDFSGN-----DAIGDVASAYQKAGVTGHVWQSDGITNCLLRGLSRVREAVANRDSSN-GYINKVYY
Lb3             IKASGHEELFEKIGWDFSGN-----EDLGDIRRVYQKYGIDEHIWQGDGITNCLPRGDYRLTEAMKKKNDPDYKYTEKVYT
SMase I         LKKEGHEDLLEKVGYDFSGPYLPSLPTLDATHEAYKKAGVDGHIWLSDGLTNFSPLGDMARLKEAIKSRDSANGFINKIYY
GDPD            YGSIENFVERVEKERPYSLHVPYQAFE-------LEYAVEVLRSFRKKG-------------------------I-VIFV
                230                                                  285
Lb1             WTVDKRASTRDALDAGVDGIMTNYPDVIADVLSESAYSAKFRIATYDDNPWETFKN
Lb3             WSIDKEASIRNALRLGVDAVMTNYPARVKSILNESEFSSTHRMATYEDNPWQK---
SMase I         WSVDKVSTTKAALDVGVDGIMTNYPNVLIGVLKESGYNDKYRLATYDDNPWETFKN
GDPD            WTLNDPEIYRKIRREIDGVITDEVELFVKLR-------------------------
```

Fig. 5. Multiple alignment of SMase I (GenBank Accession No. AY093599 and PDB code: 1XX1), Lb1, and Lb3 SMases D from *Loxosceles bonetti* (Accession Nos. AY559844 and AY559845, respectively) and GDPD from *Thermotoga maritima* (PDB code: 1O1Z). Amino acids involved in metal-ion binding and catalysis are boxed in light gray and cysteines are boxed in yellow. The numbers represent the SMase I sequence. (For interpretation of the references to color in this figure legend, the reader is referred to the web version of this paper.)

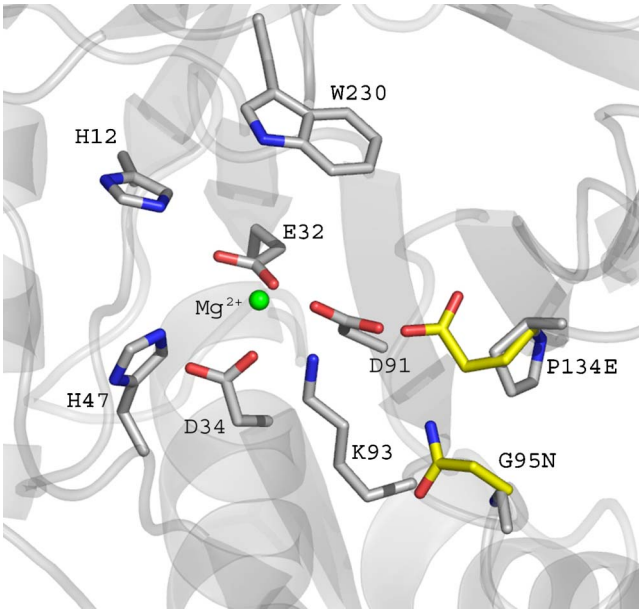

Fig. 6. Amino acid differences at the entrance to the active-site pocket of SMase D Class IIa (carbon atoms in white) and IIb (carbon atoms in yellow). (For interpretation of the references to color in this figure legend, the reader is referred to the web version of this paper.)

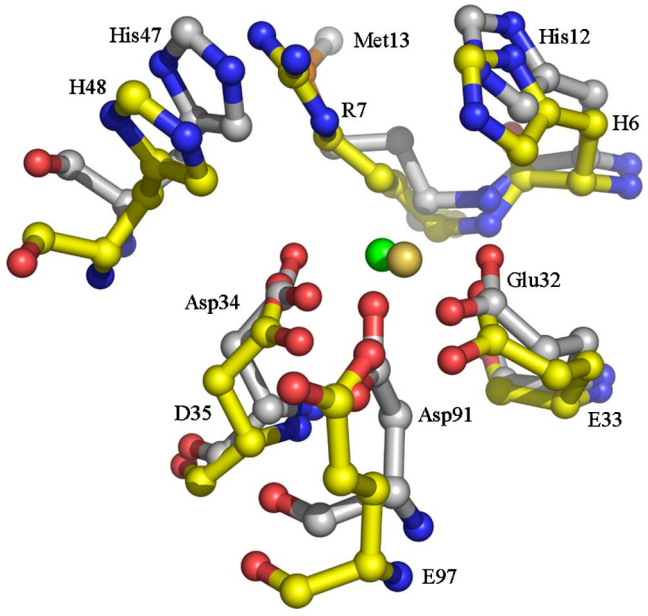

Fig. 7. Amino acid differences in the metal-ion binding and active sites of SMases I (carbon atoms in white; three letter code) and in GDPD from *Escherichia coli* (PDB code:1YDY) (carbon atoms in yellow; one-letter code). Yellow-orange and green spheres represent the Ca^{2+} and Mg^{2+} ions, respectively. (For interpretation of the references to color in this figure legend, the reader is referred to the web version of this paper.)

the stabilization of the substrate hydrocarbon tail during the catalysis event. Thus, the modifications of the local charge and hydrophobicity on the *i*-face, in the vicinity of the entrance to the active site could account for the observed lack of activity upon sphingomyelin by class IIb SMases D.

Common features of the catalytic mechanisms of SMases D and GDPDs

GDPDs encountered in bacteria, higher eukaryotes, and humans are involved in glycerol metabolism and catalyze the reaction of glicerophosphodiester and water to alcohol and *sn*-glycerol-3-phosphate. Structure based sequence alignments indicate that the SMases D and GDPDs are structurally related as pointed out earlier [23] and that the catalytic sites are highly conserved, suggesting that they evolved from a common ancestor and share a similar catalytic mechanism. SMases D are Mg^{2+}-dependent enzymes whereas GDPDs are Ca^{2+}-dependent enzymes due to the substitution of Asp91 by Glu in the latter enzymes (Fig. 7). SMases D bind Mg^{2+} both in the presence and absence of substrate analogues, however, the GDPDs only bind the metal ion simultaneously with the substrate as in the case of the bacterial neutral SMase C [24]. The catalytic mechanism of GDPDs also depend on the acid–base

reactions of two His residues (His6 and His48, based on the numbering of PDB code: 1O1Z) which are assisted by a network of hydrogen bonds in a fashion similar to that observed in the SMases D (Fig. 3C). His47 in the SMase D is hyperpolarized by a short bond to the carbonyl oxygen atom of Gly48, whereas, His48 in GDPD is hyperpolarized by an analogous bond to Asp49 OD1 (Fig. 3C). The proton donor His12 in SMase D is supported by hydrogen bonds to Asp233 and Asn252, whereas His6 in GDPD is hydrogen bonded to Asn195 and Asp213 (Fig. 3C). Additionally, the residues surrounding the catalytic site are conserved between the two enzymes except for the substitution of Met13 by Arg7 which occupies the same relative position (Fig. 7).

Conclusion

SMases D are the principal components responsible for the significant toxicity exhibited by spider venoms of the genus *Loxosceles*. These enzymes belong to the family of phosphodiesterases and serve as structural models to understand lysosomal acid and plasma membrane-bound neutral sphingomyelinases that are encountered in mammalian cells. These two important classes of phosphodiesterases form the principal pathway for sphingomyelin degradation following a reaction analogous to the reaction catalyzed by phospholipases C that yields ceramides and phosphocholine. Whereas SMases D are encountered only in spider venoms and in some bacteria being conspicuously absent in the animal kingdom, the GDPDs are widely distributed in both prokaryotes and eukaryotes and these two functionally different enzymes use the same basic structural and catalytic motifs to hydrolyze different substrates.

Acknowledgments

Financial support by FAPESP, CEPID, SMOLBNet, CNPq, CAPES/PROBAL/DAAD (415-br-probal/ale-03/17635), The Welcome Trust and FUNDUNESP are gratefully acknowledged. M.T.M is the recipient of a FAPESP fellowship.

References

[1] L.A. Van Meeteren, F. Frederiks, B.N. Giepmans, M.F. Pedrosa, S.J. Billington, B.H. Jost, D.V. Tambourgi, W.H. Moolenaar, Spider and bacterial sphingomyelinases D target cellular lysophosphatidic acid receptors by hydrolyzing lysophosphatidylcholine, J. Biol. Chem. 279 (2004) 10833–10836.
[2] A. Gomez-Munoz, Ceramide-1-phosphate: a novel regulator of cell activation, FEBS Lett. 562 (2004) 5–10.
[3] B. Anliker, J. Chun, Lysophospholipid G protein-coupled receptors, J. Biol. Chem. 279 (2004) 20555–20558.
[4] W.H. Moolenaar, L.A. van Meeteren, B.N. Giepmans, The ins and outs of lysophosphatidic acid signaling, BioEssays 26 (2004) 870–881.
[5] J.M. Futrell, Loxoscelism, Am. J. Med. Sci. 304 (1992) 261–267.
[6] M.T. Murakami, M.F. Fernandes-Pedrosa, D.V. Tambourgi, R.K. Arni, Structural basis for metal ion coordination and the catalytic mechanism of sphingomyelinases D, J. Biol. Chem. 280 (2005) 13658–13664.
[7] M.F. Fernandes-Pedrosa, I.L. Junqueira de Azevedo, R.M. Goncalves-de-Andrade, C.W. van den Berg, C.R. Ramos, P.L. Ho, D.V. Tambourgi, Molecular cloning and expression of a functional dermonecrotic and hemolytic factor from *Loxosceles laeta* venom, Biochem. Biophys. Res. Commun. 298 (2002) 638–645.
[8] D.I. Svergun, C. Barbareto, M.H.J. Koch, CRYSOL—a Program to evaluate X-ray solution scattering of biological macromolecules from atomic coordinates, J. Appl. Crystallogr. 28 (1995) 768–773.
[9] Z. Otwinowski, W. Minor, Processing of X-ray diffraction data collection in oscillation mode, Methods Enzymol. 276 (1997) 307–326.
[10] A.A. Vaguine, J. Richelle, S.J. Wodak, SFCHECK: a unified set of procedures for evaluating the quality of macromolecular structure-factor data and their agreement with the atomic model, Acta Crystallogr. D Biol. Crystallogr. 55 (1999) 191–205.
[11] T.O. Yeates, Detecting and overcoming crystal twinning, Methods Enzymol. 276 (1997) 344–358.
[12] J. Navaza, AMoRe: an automated package for molecular replacement, Acta Crystallogr. sect. A 50 (1994) 157–163.
[13] G.N. Murshudov, A.A. Vagin, E.J. Dodson, Refinement of macromolecular structures by the maximum-likelihood method, Acta Crystallogr. Sect. D 53 (1997) 240–255.
[14] T.A. Jones, Interactive computer graphics: FRODO, Methods Enzymol. 115 (1985) 157–171.
[15] P. Emsley, K. Cowtan, Coot: model-building tools for molecular graphics, Acta Crystallogr. Sect. D 60 (2004) 2126–2132.
[16] A. Perrakis, R. Morris, V.S. Lamzin, Automated protein model building combined with iterative structure refinement, Nat. Struct. Biol. 6 (1999) 458–463.
[17] R.A. Laskowski, M.W. MacArthur, D.S. Moss, J.M. Thornton, PROCHECK: a program to check the stereochemical quality of protein structures, J. Appl. Crystallogr. 26 (1993) 283–291.
[18] A. Sali, T.L. Blundell, Comparative protein modelling by satisfaction of spatial restraints, J. Mol. Biol. 234 (1993) 779–815.
[19] A. Fiser, R.K. Do, A. Sali, Modeling of loops in protein structures, Protein Sci. 9 (2000) 1753–1773.
[20] G.N. Ramachandran, C. Ramakrishnan, V. Sasisekharan, Stereochemistry of polypeptide chain configurations, J. Mol. Biol. 7 (1963) 95–99.
[21] G. Newlands, C. Isaacson, C. Martindale, Loxoscelism in the Transvaal. South Africa, Trans. R. Soc. Trop. Med. Hyg. 76 (1982) 610–615.
[22] D.V. Tambourgi, M. Fernandes-Pedrosa, C.W. Van den Berg, R.M. Goncalves-de-Andrade, M. Ferracini, D. Paixao-Calvacante, B.P. Morgan, N.K. Rushmere, Molecular cloning, expression, function and immunoreactivities of members of a gene family of sphingomyelinases from *Loxosceles* venom glands, Mol. Immunol. 41 (2004) 831–840.
[23] M.H. Cordes, G.J. Binford, Lateral gene transfer of a dermonecrotic toxin between spiders and bacteria, Bioinformatics 22 (2005) 264–268.
[24] A.E. Openshaw, P.R. Race, H.J. Monzo, J.A. Vazquez-Boland, M.J. Banfield, Crystal structure of SmcL, a bacterial neutral sphingomyelinase C from Listeria, J. Biol. Chem. 280 (2005) 35011–35017.